

Learning curve of a robotic-assisted bronchoscopy system in sampling peripheral pulmonary nodules

Fangfang Xie^{1,2}, Qin Zhang^{1,2}, Shuaiyang Liu^{1,2}, Lijun Yan^{1,2}, Yongzheng Zhou^{1,2}, Jiayuan Sun^{1,2}

¹Department of Respiratory Endoscopy, Department of Respiratory and Critical Care Medicine, Shanghai Chest Hospital, School of Medicine, Shanghai Jiao Tong University, Shanghai 200030, China;

²Shanghai Engineering Research Center of Respiratory Endoscopy, Shanghai 200030, China.

To the Editor: Computed tomography (CT) has been used for the screening of lung cancer in high-risk populations, with a subsequent reduction in lung cancer-related mortality.^[1] However, it has also resulted in a considerable increase in the discovery of peripheral pulmonary nodules (PPNs), which require further diagnosis. Conventional bronchoscopy is used to biopsy lung tissues from the endoluminal route to ensure minimum invasion. However, reaching the periphery of the lung is challenging because of the relatively large diameter of the bronchoscope, which limits the diagnostic value of bronchoscopy for PPNs. Although various advanced bronchoscopic techniques have been developed to improve PPN diagnosis, the pooled diagnostic yield is only 70%,^[2] which indicates that diagnostic accuracy can still be improved. Robotic-assisted bronchoscopy systems may be an alternative solution for addressing these limitations. The IONTM system (Intuitive Surgical, Inc., Sunnyvale, CA, USA) is a robotic-assisted bronchoscopy platform that uses shape-sensing technology, which significantly increases the ability to localize and puncture small PPNs.^[3] However, few studies have evaluated the use of this system in the Chinese population.

A multicenter prospective study was initiated in China and registered on the Chinese Clinical Trial Registry (ChiCTR2100049565) platform to evaluate the feasibility of using the IONTM system in PPN biopsy. The study is still ongoing. Here we report the early results of this study, specifically those obtained via the analysis of the learning curve by a single physician at a single center. The study protocol was approved by the institutional ethics committee of Shanghai Chest Hospital (No. LS2107). All patients participating in the study provided written informed consent.

This prospective, single-arm study was conducted at our center between July and October 2021. This study enrolled a total of 30 patients with PPNs with a diameter ranging from 8 to 30 mm that were suspected to be malignant. All IONTM procedures were performed under general anesthesia with endotracheal intubation. A 1.4-mm radial endobronchial ultrasound (r-EBUS) mini probe was used to confirm the location of the nodule. Sampling tools, including the Flexision biopsy needle, biopsy forceps, and cytology brush, were used under fluoroscopy to collect samples. Rapid on-site evaluation was performed using the obtained samples to provide feedback to physicians and determine whether the biopsy could be stopped during the procedure. All patients were examined using fluoroscopy immediately and 1 to 4 hours after the procedure to check for pneumothorax. The total cumulative fluoroscopy time was recorded, including the total fluoroscopy time during the procedure and fluoroscopy examination time immediately after the procedure. The patients were followed up at 10 ± 3 and 30 ± 7 days after the procedure. The samples obtained via the IONTM procedures were subjected to cytological and histopathological assessments. The final diagnosis was made by the physician based on the available information until the last follow-up.

The cumulative sum (CUSUM) method was used for the quantitative evaluation of the learning curve based on the operation time,^[4] including registration, navigation, and total procedure time. The registration time was defined as the time from the insertion of the catheter to the time when aligning the three-dimensional plan to the patient's anatomy was completed. The navigation time was defined as the time from catheter started from the main trachea to the time when the catheter was parked and ready for r-EBUS

Access this article online

Quick Response Code:



Website:
www.cmj.org

DOI:
10.1097/CM9.0000000000002304

Correspondence to: Dr. Jiayuan Sun, Department of Respiratory Endoscopy, Department of Respiratory and Critical Care Medicine, Shanghai Chest Hospital, School of Medicine, Shanghai Jiao Tong University, 241 West Huaihai Road, Shanghai 200030, China
E-Mail: xkyjysun@163.com

Copyright © 2022 The Chinese Medical Association, produced by Wolters Kluwer, Inc. under the CC-BY-NC-ND license. This is an open access article distributed under the terms of the Creative Commons Attribution-Non Commercial-No Derivatives License 4.0 (CCBY-NC-ND), where it is permissible to download and share the work provided it is properly cited. The work cannot be changed in any way or used commercially without permission from the journal.

Chinese Medical Journal 2022;135(22)

Received: 27-03-2022; Online: 27-12-2022 Edited by: Peifang Wei

or sampling tool insertion. The total procedure time was defined as the time from catheter insertion into the endotracheal tube to catheter removal. The CUSUM learning curve was then fitted, and the fitting model was assessed using *P* value and *R*² coefficient. The value of the X-axis corresponding to the peak of the curve represented the minimum number of cases required to accumulate across the learning curve.

CUSUM was also used to analyze the learning curve based on a successful diagnostic procedure, as reported previously.^[5] In the present study, we noted an acceptable failure ratio (*p*₀) of 0.2 and an unacceptable failure ratio (*p*₁) of 0.4. Standard type I error (α) and standard type II error (β) were set at 0.1. A CUSUM line below the acceptable failure rate boundary (*h*₀) represented proficiency. According to the assumptions, 24 procedures are required to verify *p*₀ and 20 to verify *p*₁.

In total, 30 patients with a median age of 63.5 years old were enrolled in this study [Supplementary Table 1, <http://links.lww.com/CM9/B213>]. Of the 30 nodules, 20 (66.7%) and 13 (43.3%) were present in the upper lobes and outer one-third area of the lung, respectively. CT bronchus sign was present in 23 (76.7%) nodules. The average nodule diameter was 17.1 ± 4.3 mm, 16.9 ± 5.7 mm, and 16.7 ± 4.8 mm in the axial, coronal,

and sagittal plans, respectively. The average/median operation time was 3.4 ± 1.2 min, 3.5 (2.0, 11.0) min, 40.7 ± 18.0 min, and 7.1 ± 3.3 min for registration, navigation, total procedure, and total cumulative fluoroscopy time, respectively. The r-EBUS view was obtained in 29 (96.7%) nodules before the first attempt at sampling; of the 29 nodules, 14 (46.7%) were concentric. An overall concentric view was obtained in 21 (70.0%) nodules before and/or during the sampling attempts. Supplementary Table 2 (<http://links.lww.com/CM9/B213>) summarizes the nodule and procedure characteristics, and Supplementary Figure 1 (<http://links.lww.com/CM9/B213>) shows a case of a patient undergoing the IONTM procedure.

Of the 30 nodules, pathology examinations of the specimen obtained via the IONTM procedure revealed that 26 were malignant, one was benign, two were with atypical cells only, and one was normal lung tissue. The final diagnoses of these patients were non-small cell lung cancer (23, 76.7%), extrathoracic tumor metastasis (6, 20.0%), and organizing pneumonia (1, 3.3%). The diagnostic yield of the IONTM procedures performed in this study was 90.0%. Twenty-seven and 3 out of the 30 IONTM procedures were diagnostic and nondiagnostic, respectively. Of the 29 patients diagnosed with malignancy, 26 were diagnosed using the IONTM procedure, resulting in a sensitivity of 90% for malignancy. The

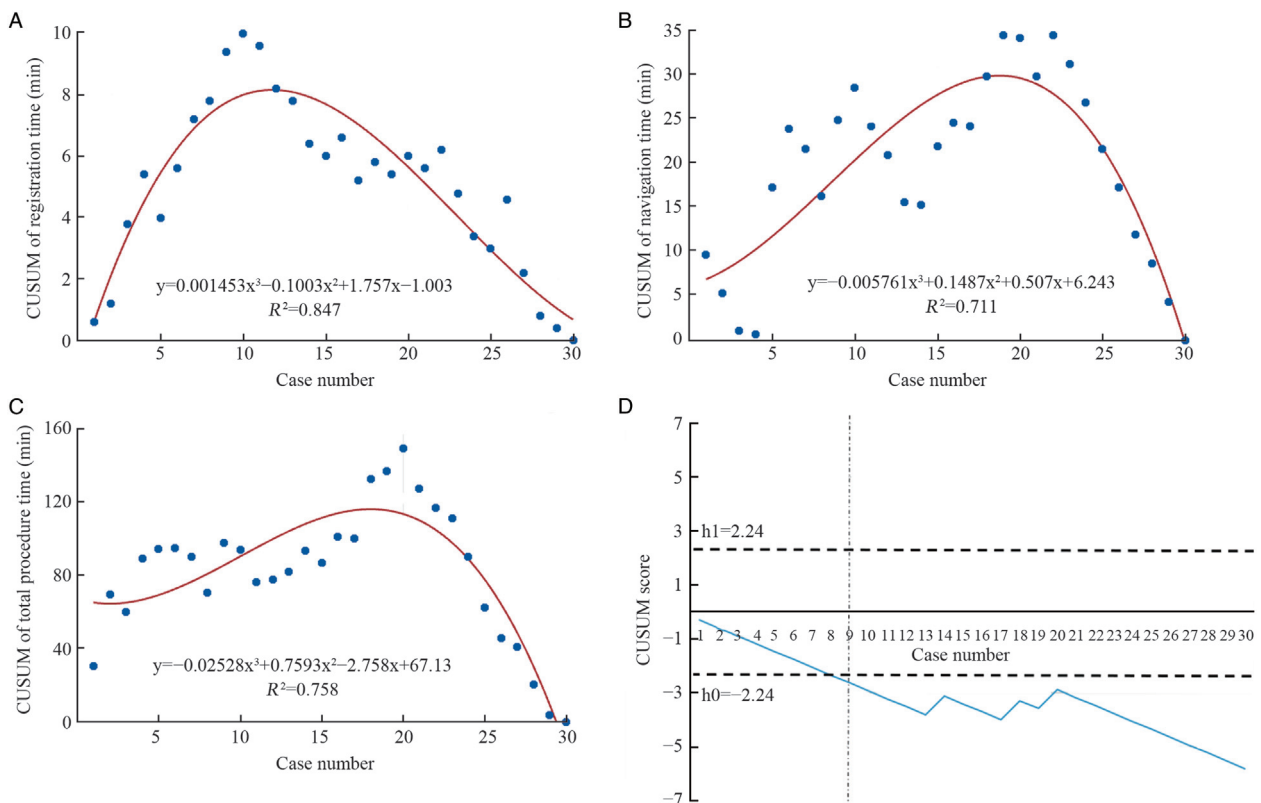


Figure 1: CUSUM learning curve analysis. (A) CUSUM of registration time in relation to case number. The red solid line represents the fitting curve of the best fitting model as a third-order polynomial with an $R^2 = 0.847$; $n = 30$. (B) CUSUM of navigation time in relation to case number. The red solid line represents the fitting curve of the best fitting model; $n = 30$. (C) CUSUM of total procedure time in relation to case number. The red solid line represents the fitting curve of the best fitting model; $n = 30$. (D) CUSUM analysis curve based on successful diagnostic procedure. The blue line indicates the CUSUM of diagnostic yield. The horizontal dotted lines represent the unacceptable failure rate boundary line *h*₁ (above) and acceptable failure rate boundary line *h*₀ (below). The physician attained competence immediately and passed lower decision boundary (*h*₀) at the 9th case (the vertical dotted line) meaning statistically significant improvement in performance. CUSUM: Cumulative sum.

factors that might affect the diagnostic performance of the ION™ procedures were analyzed via univariable analysis. The results of the analysis showed that the only two factors associated with the diagnostic performance of the ION™ procedure were the r-EBUS view before the first sampling attempt and achievement of a concentric r-EBUS view before and/or during samplings ($\chi^2 = 10.952$, $P = 0.022$ and $P = 0.021$ [Fisher's exact test]). No pneumothorax, pneumonia, airway bleeding, or other complication was reported.

The operation time for each ION™ procedure was plotted in a chronological manner. The registration learning curve was plotted using the best-fitting model as a third-order polynomial with a high R^2 value of 0.847 [Figure 1A]. The registration learning curve can be divided into two phases, cases 1 to 12 and cases 13 to 30, with case 12 marking the peak of the curve. Similarly, the navigation learning curve was fitted using the best-fitting model as a third-order polynomial with a high R^2 value of 0.711 [Figure 1B]. The navigation learning curve peaked at case 18, which divided the curve into two phases: cases 1 to 18 and cases 19 to 30. The CUSUM learning curve based on the total procedure time was fitted using the best-fitting model as a third-order polynomial with a high R^2 value of 0.758 [Figure 1C], which was divided into two phases: cases 1 to 18 and cases 19 to 30. A stable total procedure time was achieved after 18 cases, which divided the learning curve into two phases. The baseline and procedure characteristics as well as diagnostic yields were compared between the two phases of the learning curve; the results showed no statistical significance, except for sex (male, 8/18 *vs.* 12/12, $P = 0.021$ [Fisher's exact test]). The total procedure (48.1 ± 17.8 min *vs.* 29.7 ± 11.9 min, $t = 3.135$, $P = 0.004$) and total cumulative fluoroscopy time (8.1 ± 3.6 min *vs.* 5.5 ± 2.2 min, $t = 2.445$, $P = 0.021$) significantly decreased after 18 cases. The CUSUM of the successful diagnostic procedure revealed that the physician attained competence immediately and the curves remained below the predetermined upper decision boundary ($h1 = 2.24$) throughout the study period. In addition, the graph crossed the lower decision boundary at case 9 during the study period [Figure 1D], indicating that proficiency was obtained.

This study investigated the learning curve of a robotic-assisted bronchoscopy system. We conducted CUSUM analysis based on operation time. A single physician achieved stable registration, navigation, and total procedure time after 12, 18, and 18 cases, respectively. Registration is a relatively simpler procedure than navigation and biopsy as no subtle anatomy is involved. This is probably why fewer cases were needed to pass the learning curve of registration than those needed for navigation or the entire procedure. The baseline characteristics and diagnostic yields of the two phases divided by case 18 showed no statistically significant difference, except for sex. The total procedure and total cumulative fluoroscopy time decreased significantly after 18 cases, indicating that the operator was proficient.

Our study showed high diagnostic yield and sensitivity for PPN malignancy, suggesting that promising diagnostic accuracy can be achieved by experienced bronchoscopists, even as beginner users of ION™ technology. The analysis of the CUSUM learning curve based on the successful diagnostic procedure also revealed that a beginner user attained competence immediately, indicating that the diagnostic yield was stable. The graph crossed the lower decision boundary, suggesting that the diagnostic yield improved gradually. In our study, the diagnostic yield was affected only by the factors of r-EBUS view, which was highly dependent on the accessibility, accuracy, and stability of the ION™ system because of the fact that the CT bronchus sign was not a factor affecting the diagnostic yield. This is because these features of the ION™ system ensured that the operator can attain competence immediately. No adverse event was reported during or after the procedure in our study.

Our study reports the experience of only a single physician at a single center. The learning curve must be explored at multiple centers with diversified users. Our study was further limited by the small sample size and short follow-up duration. Future studies with a larger sample size and longer follow-up duration may reveal additional phases of the learning curve based on both operation time and diagnostic performance.

In conclusion, our study demonstrated that the ION™ system is a promising approach for PPN diagnosis, with encouraging diagnostic yield and safety profile. A stable total procedure time was achieved by a single physician after 18 cases. A beginner may attain competence regarding a stable diagnostic yield immediately and improve gradually.

Conflicts of interest

None.

References

1. Oudkerk M, Liu S, Heuvelmans MA, Walter JE, Field JK. Lung cancer LDCT screening and mortality reduction - evidence, pitfalls and future perspectives. *Nat Rev Clin Oncol* 2021;18:135–151. doi: 10.1038/s41571-020-00432-6.
2. Wang Memoli JS, Nietert PJ, Silvestri GA. Meta-analysis of guided bronchoscopy for the evaluation of the pulmonary nodule. *Chest* 2012;142:385–393. doi: 10.1378/chest.11-1764.
3. Benn BS, Romero AO, Lum M, Krishna G. Robotic-assisted navigation bronchoscopy as a paradigm shift in peripheral lung access. *Lung* 2021;199:177–186. doi: 10.1007/s00408-021-00421-1.
4. Zhang T, Zhao ZM, Gao YX, Lau WY, Liu R. The learning curve for a surgeon in robot-assisted laparoscopic pancreaticoduodenectomy: a retrospective study in a high-volume pancreatic center. *Surg Endosc* 2019;33:2927–2933. doi: 10.1007/s00464-018-6595-0.
5. Orhan-Sungur M, Altun D, Özkan-Seyhan T, Aygün E, Koltka K, Çamcı E. Learning curve of ultrasound measurement of subglottic diameter for endotracheal tube selection in pediatric patients. *Paediatr Anaesth* 2019;29:1194–1200. doi: 10.1111/pan.13751.

How to cite this article: Xie F, Zhang Q, Liu S, Yan L, Zhou Y, Sun J. Learning curve of a robotic-assisted bronchoscopy system in sampling peripheral pulmonary nodules. *Chin Med J* 2022;135:2753–2755. doi: 10.1097/CM9.0000000000002304